Supplemental Figure Legends

Figure S1: Digestion and Sequencing controls confirm efficient oxidation and bisulfite conversion. a) Spike-in digestion control sequences contain a 5hmC mark at the TCGA Taq α1 restriction enzyme digestion site. An efficient oxidation reaction will convert this 5hmC to thymine after bisulfite conversion, which will prevent the enzyme from cutting. In the bisulfite-alone reaction, the 5hmC will remain a cytosine after the bisulfite reaction and will be cut by the enzyme. Digestion control reactions were run with (+) and without (-) the restriction enzyme and an additional cutting control was included, also with (+) and without (-) the restriction enzyme. Using targeted bisulfite sequencing, we also interrogated spiked-in sequencing controls that contain a variety of 5hmC, 5mC, 5fC, and C bases. Conversion rates of cytosine to thymine in for the oxBS (b) and BS (c) reactions were as expected, with 5hmC being converted to thymine after oxidation and bisulfite conversion.

Figure S2: The bisulfite conversion reagents in the TrueMethyl kit perform similar to those from Zymo Research. DNA from the same cerebellum samples was converted using reagents from either Zymo Research or Cambridge Epigenetix. Both samples were run on independent Infinium methylationEPIC arrays and produced strongly correlated 5mC (β_{BS}) data ($r = 0.99$; $p < 0.05$).

Figure S3: Quality control data show the proper functioning of that Infinium methylationEPIC arrays. a) The total signal from each sample on the array was consistent between tissue types and treatments. A fully methylated sequence (HCTT116_methylated) was added to the array as a positive control. b) Unsupervised hierarchical clustered samples not only by tissue type but also by treatment (oxBS vs BS alone). c) Similarly, multidimensional scaling also showed distinct clustering of single by tissue type. Given the more highly abundant 5hmC signal in the cerebellum, clustering based on treatment was only seen in this tissue type.

Figure S4: The abundance of 5hmC-containing probes shows strong tissue-specific variability. a) There exists a very small overlap of detectable 5hmC probes across the tissue types, likely as a result of the low abundance of 5hmC in peripheral tissues. b) The overlap of 5mC-containing probes is much stronger, with more than 90% overlap of probes showing detectable 5mC in blood, cerebellum, and saliva. Of the 2,528 probes with detectable 5hmC common in all tissues, (c) $\Delta\beta_{(BS-OX)}$ values ranged from 0.0799 (dashed line) to slightly more than 0.25 in blood and saliva and exceeded 0.50 in cerebellum. Similarly, these probes scattered across all chromosomes (d), were present in gene bodies and intergenic regions (e), and were more abundant in Fantom5 enhancers compared to DNase hypersensitivity sites and regions of open chromatin (f).

Figure S5: The fraction of probes containing detectable 5mC and 5hmC is correlated with the density of genes on the chromosome. A negative correlation exists between gene density, defined as the number of genes per Mb (http://www.cshlp.org/ghg5_all/section/dna.shtml), and the fraction of probes containing detected 5mC ($p<0.0001$) or 5hmC ($p<0.01$).

Supplementary Figure S1

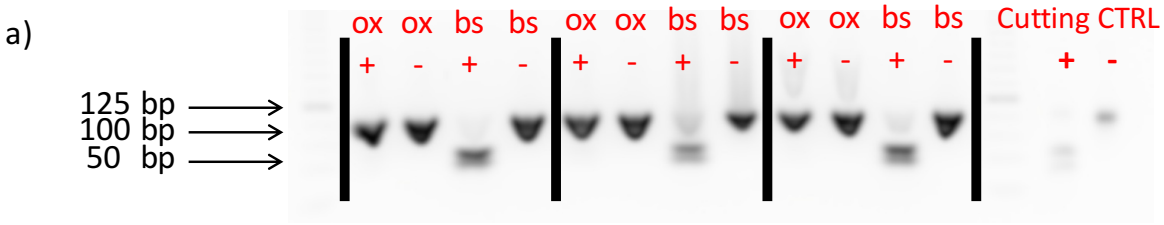

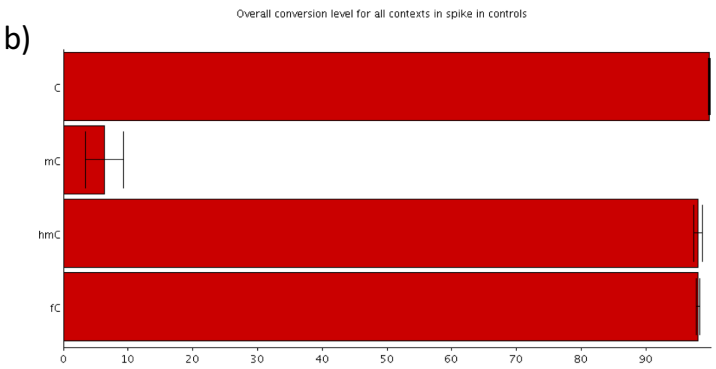

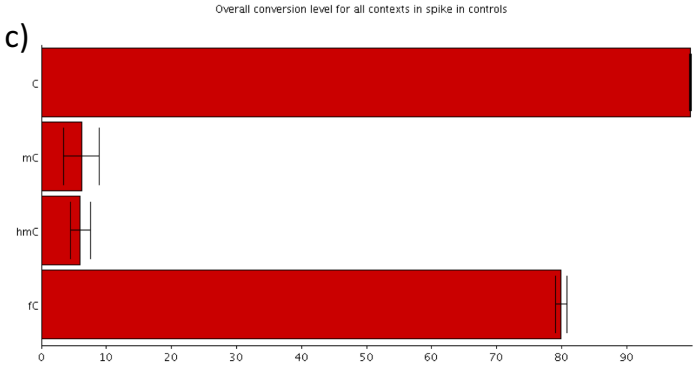

Supplementary Figure S2

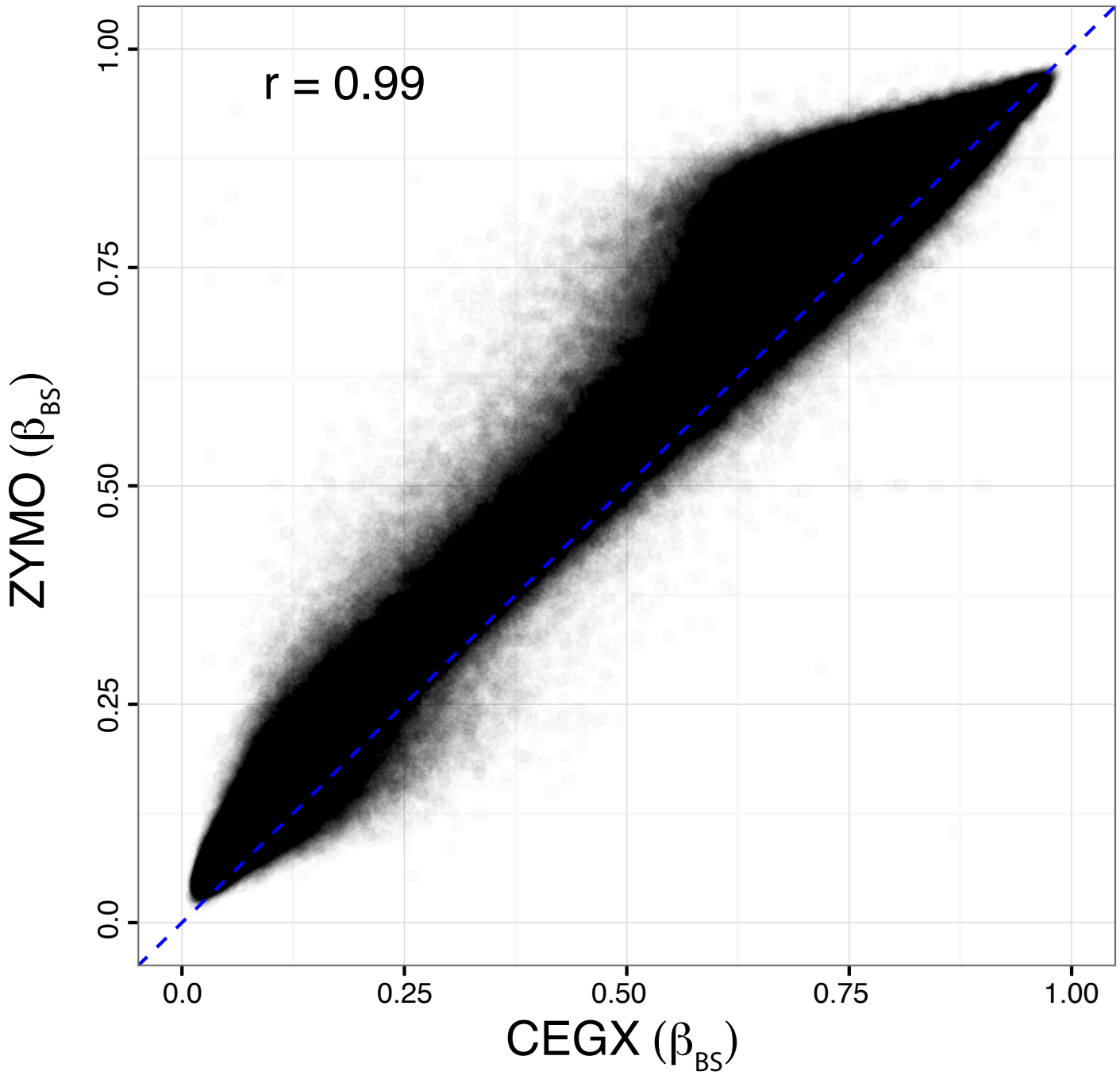

Supplementary Figure S3

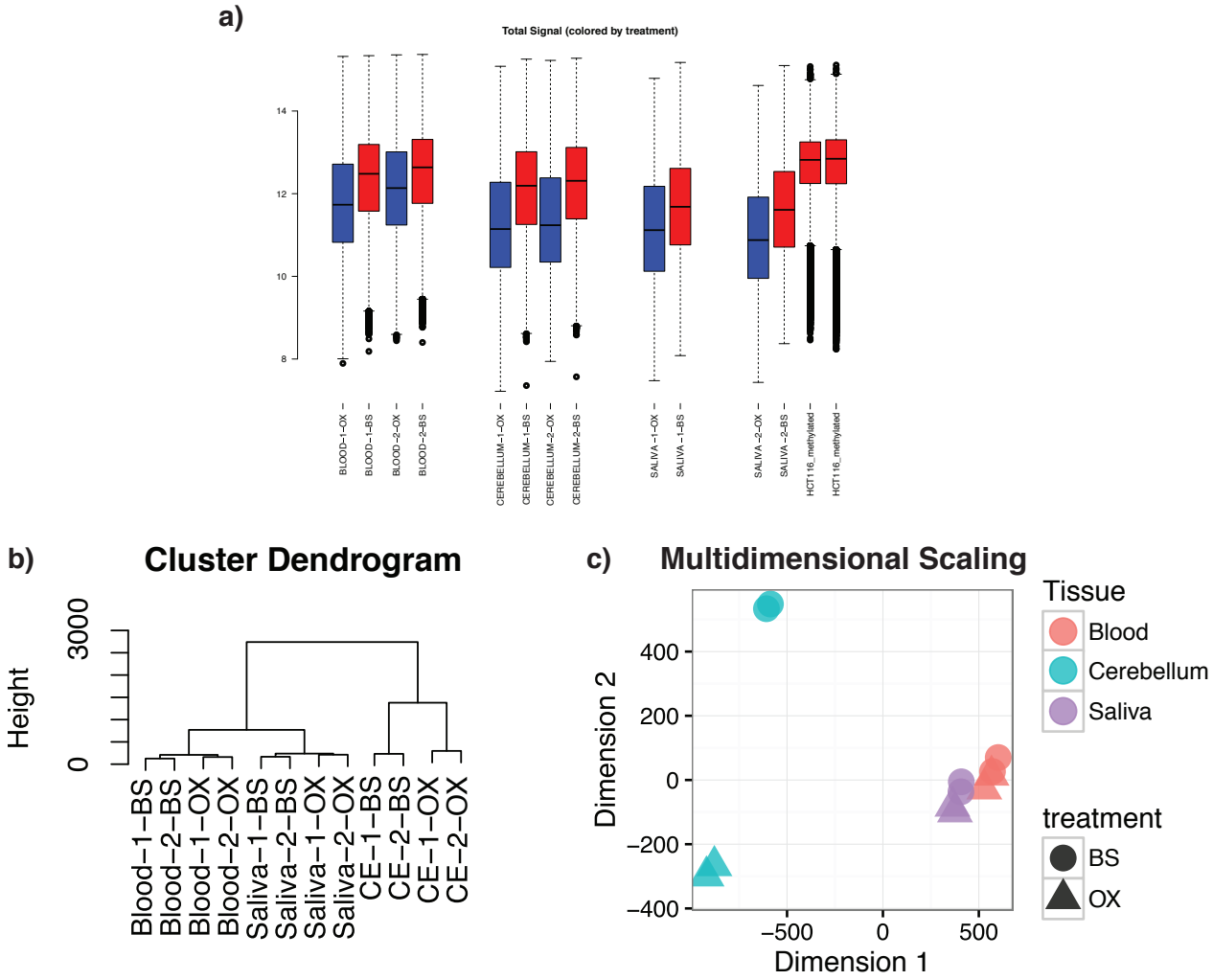

Supplementary Figure S4

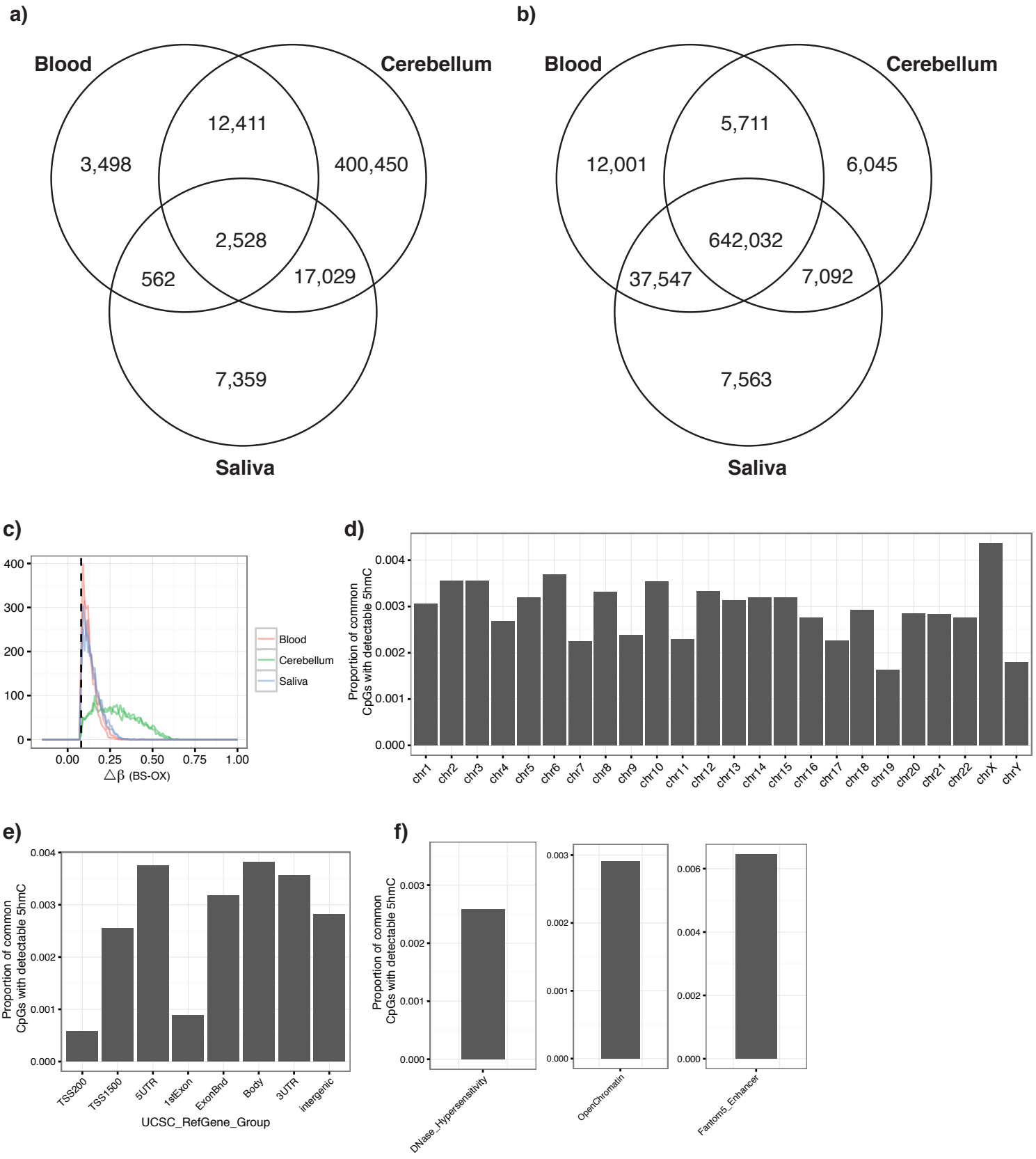

Supplementary Figure S5